Longitudinal Hall effect in $SrAs_3$

W. Bauhofer
Max-Planck-Institut für Festkörperforschung, Heisenbergstrasse 1, D-7000 Stuttgart 80, Federal Republic of Germany
(Received 26 December 1984)

An unusual first-order Hall effect with the magnetic field parallel either to the current or to the Hall field is observed in monoclinic semimetallic $SrAs_3$. Data are presented showing the dependence of this longitudinal Hall effect (LHE) on orientation, temperature, and magnetic field strength. Both symmetry-allowed longitudinal components have been measured and are of the same order of magnitude as the transverse or normal Hall effect. The signs of the longitudinal Hall components are determined using samples with well-defined c orientations. The occurrence of a LHE cannot be explained within a simple one-band model of conductivity. For monoclinic symmetry, however, nonvanishing longitudinal coefficients are derived from a two-band model.

I. INTRODUCTION

In a recent paper (which we will denote as paper I) we have reported the observation of a first-order longitudinal Hall effect (LHE) in $SrAs_3$. In the usual Hall geometry, the electrical current, magnetic field, and Hall electrical field are mutually perpendicular (in this paper further referred to as THE, denoting a transverse Hall effect) since the Lorentz force acts perpendicularly to the velocity of the charge carriers and to the applied magnetic field. However, strict orthogonality holds exactly only for freely moving particles. In crystals of low symmetry, first-order LHE's with the magnetic field either parallel to the current or to the Hall field are possible. Paper I gave experimental evidence of the existence of LHE's in monoclinic, semimetallic $SrAs_3$.

This paper presents a detailed study of the LHE including the dependences on angle, temperature and magnetic field. The results essentially confirm our earlier statements:[1] the existence of a LHE in $SrAs_3$ in accordance with the selection rules imposed by symmetry, and a strong increase of the LHE components below ~ 150 K.

A significant observation in earlier measurements on $SrAs_3$ was an almost temperature-independent resistivity.[2] Such a behavior is often encountered in strongly disturbed low-mobility metals. In $SrAs_3$, however, it is due to a delicate balance between an increase of mobility and a reduction of charge carriers upon cooling. Therefore, slight and unintentional changes in sample preparation can have a drastic influence on the low-temperature conductivity. All samples used in this study were cut from the same Bridgman-grown crystal and show an almost identical temperature dependence of resistivity which is, at temperatures $\lesssim 100$ K, markedly different from that of the earlier grown crystals (see Fig. 3). The much higher mobility (up to 2×10^5 cm^2/V s) of the new batch of samples makes it necessary to use magnetic fields smaller than 1 kG to stay within the low-field limit which is the basis of a power series expansion of the resistivity ρ in B. The measurements of paper I were done at 8 kG which is in the intermediate field region (see Sec. IV E). The maximum around 70 K in the temperature dependence of the LHE components (as reported in paper I) is shown to arise only for intermediate magnetic fields. In the low-field limit I find a continuous increase of the absolute values of all Hall components down to the lowest temperatures.

Due to difficulties with exact sample adjustment I have adopted a precise method for determining the positions where LHE and THE should be measured. Using this method, all equivalent LHE components are found to be identical within the experimental accuracy. The inconsistency between the equivalent LHE components ρ_{232} and ρ_{322} reported in paper I seems to be caused by misalignments. Thus, the explanation for this inconsistency given in paper I is not correct.

The sample preparation and the Hall effect setup are described in Sec. II of this paper. Section III deals with the Hall tensor for monoclinic symmetry. A review is given of how all nonvanishing Hall components can be determined using differently oriented samples. The experimental results are summarized in Sec. IV. A simple two-band model which explains the occurrence of a LHE on the basis of the existence of nonvanishing off-diagonal conductivity components is presented in Sec. V.

II. EXPERIMENTAL

Single crystals of $SrAs_3$ were prepared as originally proposed by Wittmann.[2] The orientation of the samples with respect to the a and b axes was done by Laue back reflection technique. The determination of the direction of the c axis, however, requires the use of a four-circle diffractometer. Samples of typical dimensions $0.5\times 1\times 6$ mm^3 were cut with two sets of edges parallel to the a and b axes, respectively. Five probes of 100 μm gold wire were spot welded directly on the polished surfaces. $SrAs_3$ has an easy cleavage parallel to the ab plane which frequently causes cracks during the first cooling cycle when the ab plane is not parallel to the substrate. Most of the measurements were done while cooling down to save the data before a possible sample break.

The transport measurements were performed with a fully automated experimental setup shown schematically in Fig. 1. An enormous amount of data arises from the

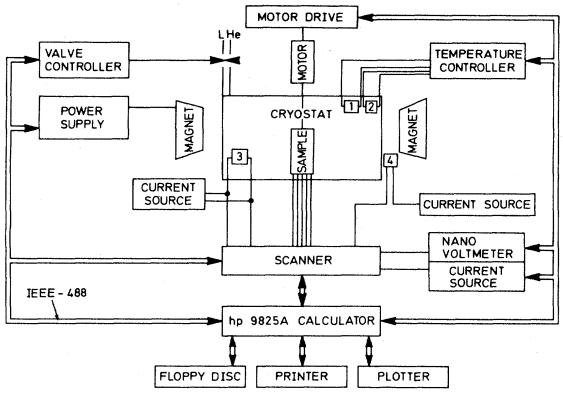

FIG. 1. Block diagram of the Hall apparatus.

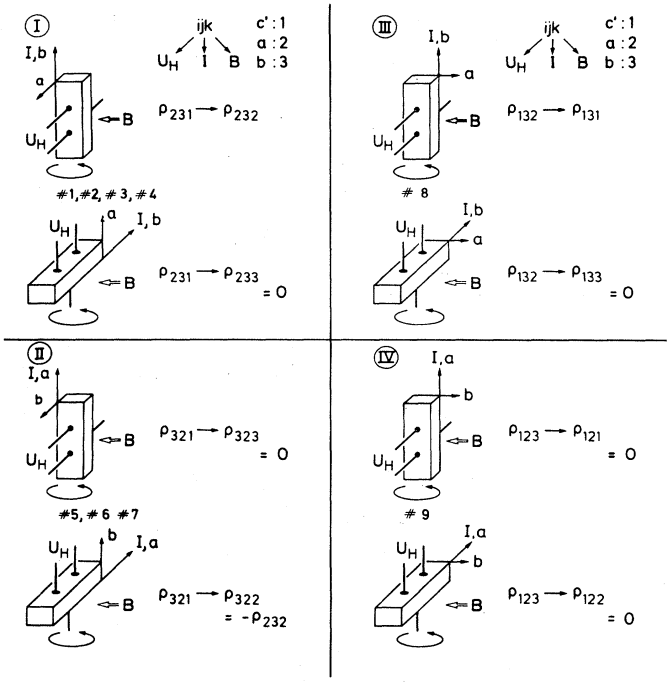

FIG. 2. Geometrical arrangements for the measurement of THE and LHE by rotating differently oriented samples in the external magnetic field **B**. The inset in the upper right corner illustrates the assignment of the Hall tensor indices to Hall voltage U_H, current I, and magnetic field B, and the adjustment of the reference frame with respect to the crystallographic axes. The direction perpendicular to the ab plane is denoted by c'. Sample numbers are added to the corresponding orientation.

variation of three parameters (temperature, magnetic field **B** and angle between **B** and current or Hall field) and the reversal of current and **B**. Under optimized conditions, a measurement at stabilized temperature and fixed **B** with a 220° rotation of the sample in steps of 10° takes about 30 min. This paper summarizes the results of more than 300 h of net measurement time.

Temperature variation was achieved by controlling the He gas flow through an evaporation-type cryostat. Two different revolving sample holders were used for a rotation of the samples parallel or perpendicular to their axes, respectively.

III. SAMPLE ORIENTATION AND GEOMETRY OF LHE MEASUREMENTS

In the low-magnetic-field limit, the resistivity $\rho(\mathbf{B})$ can be expanded in powers of B (see, for example, Ref. 3):

$$\rho_{ij}(B)=\rho^0_{ij}+\rho^0_{ijk}B_k+\rho^0_{ijkl}B_kB_l+\cdots , \tag{1}$$

where ρ^0_{ij} is the zero-field resistivity, ρ^0_{ijk} the Hall tensor, and ρ^0_{ijkl} the magnetoresistivity. Higher orders in **B** will be neglected. The Onsager relations[4] as well as the crystal symmetry reduce the number of independent tensor elements. Independent first-order longitudinal components of the Hall tensor with $\mathbf{B}||\mathbf{E}_H$ or $\mathbf{B}||\mathbf{j}$ ($\mathbf{E}_H$ is the Hall electrical field, **J** the current density) exist only for low symmetries.

$SrAs_3$ crystallizes in the monoclinic space group $C2/m$. The Hall tensor for this symmetry contains three independent transverse, ρ^0_{213}, ρ^0_{132}, and ρ^0_{321}, and two independent longitudinal components, ρ^0_{232} and ρ^0_{131}.[3] The orthogonal laboratory system x_1,x_2,x_3 is adjusted to the crystallographic axes c,a,b with x_2 parallel to a and x_3 parallel to b. In this notation, b is the twofold axis and the monoclinic angle β ($=112°$ for $SrAs_3$) is between a and c.

Figure 2 illustrates how the five Hall components ρ^0_{ijk} can be measured with four differently oriented samples by rotating the samples with respect to the magnetic field **B**. For sample orientations I, II, and III, one rotation scheme always yields the sum of a THE and a LHE, whereas the other one gives a pure THE. Both effects can be separated in the following way. First, the transverse component ρ_T is determined using the geometrical arrangement showing a pure THE, then the longitudinal component ρ_L is derived from a measurement of the *same* sample in the other geometry.

The sum ρ_H of THE and LHE should, as a function of rotation angle α, behave as

$$\rho_H=\rho_T\cos\alpha+\rho_L\cos(90-\alpha) \tag{2a}$$

$$=\rho_T\cos\alpha+\rho_L\sin\alpha \tag{2b}$$

$$=\rho_T\left[\cos\alpha\pm\left|\frac{\rho_L}{\rho_T}\right|\sin\alpha\right] \tag{2c}$$

$$=(\rho_T^2+\rho_L^2)^{1/2}\cos\left[\alpha\mp\arctan\left|\frac{\rho_L}{\rho_T}\right|\right] . \tag{2d}$$

The determination of ρ_T and ρ_L from a measurement in a single geometrical arrangement depends very sensitively on the sample adjustment with respect to the magnetic field, since neither component can be found in the usual way by adjusting for maximal Hall voltage. This alignment problem explains the difference between ρ_{232} and $-\rho_{322}$ reported in paper I. We can avoid these difficulties using the above-mentioned method.

The Hall voltage goes through zero [from Eq. (2a)] at

an angle

$$\alpha_z = \arctan\left[-\frac{\rho_T}{\rho_L}\right]. \quad (3)$$

Thus, if ρ_T and ρ_L differ in their temperature variation, a temperature-dependent shift of α_z and of the position of maximal Hall voltage will occur. This behavior represents a striking deviation from regular Hall measurements where such shifts are impossible.

IV. RESULTS

This section summarizes the experimental results. The resistivities at zero magnetic field are given in Sec. IV A. The two independent LHE components ρ_{232} and ρ_{131} have to be determined from differently oriented samples and are treated separately in Secs. IV B and IV C, respectively. Section IV D deals with the THE components. All Hall components are determined by $\rho_{ijk}=(U_H)_i d/I_j B_k$ (where d is the sample thickness); ρ^0_{ijk} represents the zero-field limit: $\rho^0_{ijk}=\rho_{ijk}$ $(B\to 0)$. Typical results for the magnetic field dependences of LHE and THE components are shown in Sec. IV E.

A. Zero-field resistivities

Figure 3 shows a compilation of resistivity data of the presently used samples together with a typical curve of a sample from paper I for comparison. The low-temperature mobilities differ by about one order of magnitude. The resistivities along a, ρ^0_{22}, and perpendicular to the ab plane, ρ^0_{11}, resemble each other with respect to their magnitude and their temperature variation. The resistivity along b, ρ^0_{33}, is smaller by a factor of 5–6 than ρ^0_{22} and reveals a different temperature behavior above 100 K. Below 100 K, the temperature dependences of resistivities are isotropic which represents a remarkable contrast to the behavior of the Hall components (see Sec. IV D). The difficulties in preparing samples with their long axis perpendicular to the ab plane prevented a reliable determination of ρ^0_{12} before now.

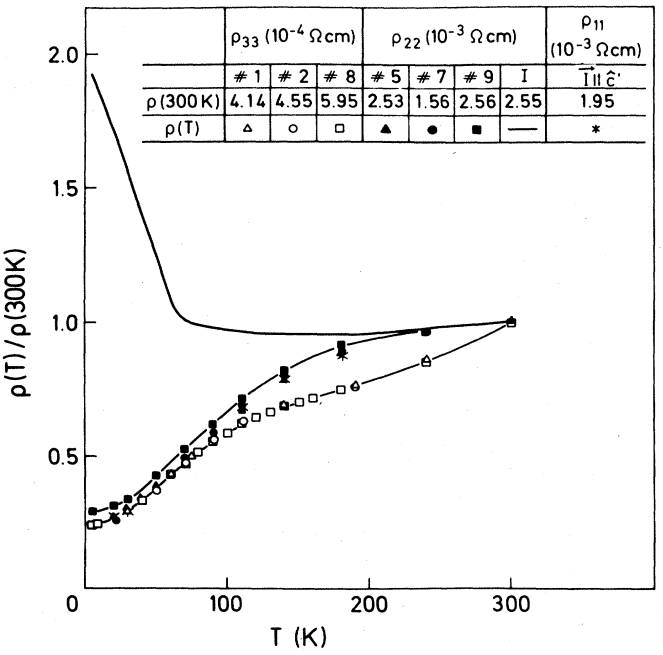

FIG. 3. Relative resistivity variation as a function of temperature of samples used in this paper compared with a typical previously measured (paper I) sample. The 300-K values are listed in the inset.

B. Temperature dependence and sign of ρ_{232}

The angular dependences of the Hall coefficients measured for one sample with orientation I in two different geometries are depicted in Fig. 4. Lines drawn at the maximal values of the pure THE curves (right-hand side) intersect equivalent curves for the other geometry (left-hand side) at the same angle for all temperatures. This angle (marked by vertical arrows) defines the correct adjustment for a pure THE in the (THE + LHE) curves. Note the different scales for ρ_H indicating a strong increase of both components with decreasing temperature. As pointed out in Sec. III, the surprising temperature-dependent shift of the sum curves is indicative of a different temperature variation of longitudinal and transverse Hall components. No shift is, of course, observed for the geometry shown on the right-hand side, giving a pure transverse Hall effect. The (THE + LHE) curves perfectly match a cosine function confirming the validity of Eq. (2).

Samples oriented as I and II (see Fig. 2) yield the same transverse and longitudinal Hall components ($\rho_{231}=-\rho_{321}$, $\rho_{232}=-\rho_{322}$) in a complementary way. Figure 5 shows a summary of the Hall components measured on two different samples of each geometry. The good agreement within the values for the LHE components (open symbols) and within the values for the THE components (filled symbols), respectively, is convincing evidence for the picture outlined in Sec. III. The measurements have been performed at 1 kG for $T>100$ K and at 0.3 kG for $T\leq 100$ K to stay within the low-field limit. The absolute values of the longitudinal components increase for decreasing B and approach a nonzero value for

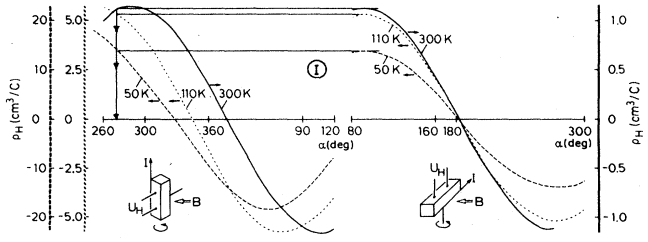

FIG. 4. Angular dependence of the Hall coefficient measured for a sample with orientation I (following the notation of Fig. 2) in two different geometries. Lines drawn at the maximal values of the right-hand curves intersect the corresponding left-hand curves at the position for a pure THE (marked by vertical arrows). Different scales in (cm^3/C) are used for ρ_H: ± 1 for $T=300$ K, ± 5 for $T=110$ K, ± 20 for $T=50$ K.

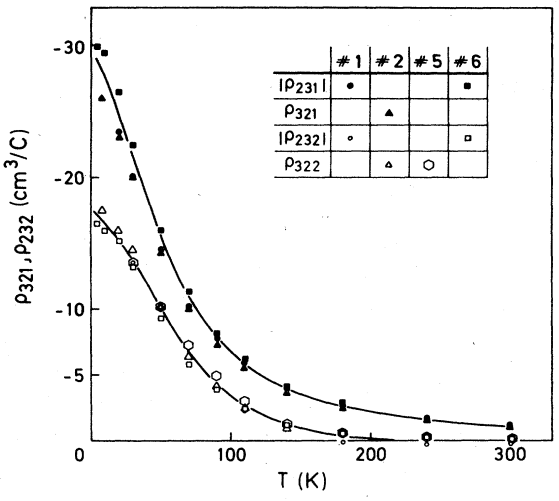

FIG. 5. Temperature dependence of Hall components obtained from differently oriented samples (see Fig. 2) in different geometrical arrangements (again see Fig. 2). The magnetic fields for samples no. 1 and no. 5 were 1 kG for $T \leq 70$ K, 3 kG for 90 K $\leq T \leq 240$ K, 8 kG for $T = 300$ K; for samples no. 2 and no. 6, 0.3 kG for $T \leq 90$ K, 1 kG for $T \geq 110$ K. The LHE components are represented by open symbols, the THE components by filled symbols. The lines merely serve as a guide to the eye.

$B \rightarrow 0$, proving them to be actually of first-order (see Sec. IV E).

The determination of the sign of the Hall components reveals an interesting difference between the transverse and longitudinal effect. The sign of a transverse component is completely determined by the direction of two crystallographic axes (a and b in our case). ρ_{321} and the other anticyclic transverse components, ρ_{213} and ρ_{132}, are found to be negative at room temperature indicating n-type conductivity.[5] ρ_{321} stays negative for $T \leq 300$ K. The sign of a longitudinal component, however, depends on the direction of the c axis, since two of the indices of a LHE component are equal. Therefore, the same sample should show an opposite shift of its zero crossings, when mounted with the c axis pointing in/out with respect to the substrate. For experimental reasons, it is more favorable to use two different samples with well-defined c orientation for this investigation. The results depicted in Fig. 6 perfectly confirm the above considerations; ρ_{232} is found to be positive.

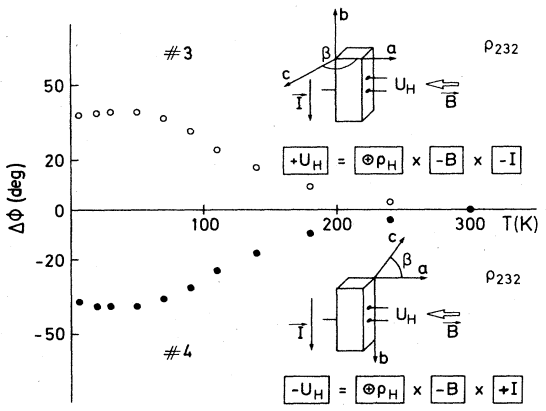

FIG. 6. Geometrical arrangement for the determination of the sign of ρ_{232}. $\Delta\phi$ denotes the shift of the temperature-dependent zero crossing of the (THE + LHE) curves with respect to the 300-K curve. The sign of U_H is found by experiment and determines the sign of ρ_H ($=\rho_{232}$ in this case).

C. Temperature dependence of ρ_{131}

The longitudinal Hall component ρ_{131} can be determined using samples with orientation III (referring again to Fig. 2). As shown in Fig. 7, these measurements reveal another surprise! The transverse component ρ_{132} passes through zero around 115 K, whereas the corresponding longitudinal component ρ_{131} does not. This means that at this temperature the usual Hall effect is turned upside down in the geometrical arrangement where (THE + LHE) is measured: The maximal Hall coefficient is detected in the longitudinal geometry whereas the normal or transverse Hall effect equals zero. The exact angular position of the LHE is again determined by the procedure explained in Sec. IV B.

Figure 8 shows the temperature variation of ρ_{132} and ρ_{131} for two different magnetic fields. ρ_{132} crosses through zero around 115 K. For $T < 115$ K, both components increasingly vary with magnetic field. This strong magnetic-field dependence is correlated with the extremely high mobilities ($\mu = 7.5 \times 10^4$ cm^2/V s at 40 K) shifting the low-field limit to rather small magnetic fields ($\mu B \approx 1$ for 1.35 kG at 40 K!). The temperature-dependent change of sign of ρ_{132} in the low-field limit is in contrast to the behavior of ρ_{213} and ρ_{321}, where a sign-reversal is only observed for $B \geq 4$ kG (see Sec. IV E).

A remarkable feature which already becomes apparent from an inspection of the left part of Fig. 7 is the fact that all curves of $(\rho_{132}\cos\alpha + \rho_{131}\sin\alpha)$ intersect for $T \leq 160$ K at the same value of $\rho_H \approx -1$ cm^3/C. Figure 9 shows that this behavior persists down to 4 K. We do not know if this "fixed point" arises accidentally or due to physical origin. From measurements on samples with well-defined c orientation, ρ_{131} is found to be positive.

D. Pure THE orientations

Sample orientation IV of Fig. 2 produces vanishing longitudinal components and indeed no LHE is observed in both geometrical arrangements. However, these measurements yield the third independent transverse component ρ_{123} whose temperature dependence is depicted in

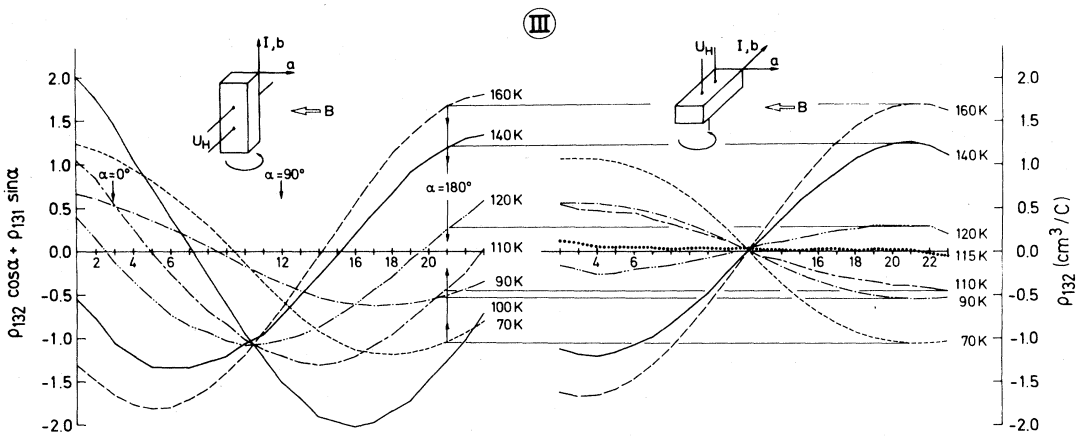

FIG. 7. Angular dependence of the Hall coefficient measured for a sample with orientation III (following the notation of Fig. 2) in two different geometries. Marks at the abscissa denote steps of 10° for the rotation angle. Lines drawn at the maximal values of the right-hand curves intersect the left-hand curves at the position of a pure THE (marked by vertical arrows at $\alpha=180°$). A pure THE is measured at $\alpha=90°$.

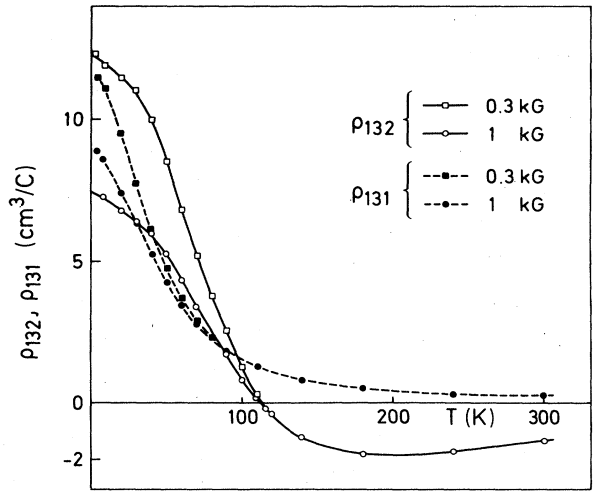

FIG. 8. Temperature dependences of transverse and longitudinal Hall components, ρ_{132} and ρ_{131}, obtained from a sample with orientation III (see Fig. 2) for two different magnetic fields.

Fig. 10. The equivalent component ρ_{213} has been obtained from measurements of a sample with $I\perp ab$ plane, $\mathbf{B}\|\hat{\mathbf{b}}$, $U_H\|\hat{\mathbf{a}}$, and the results are included in Fig. 10. The agreement is satisfactory. Samples with the long axis $\perp$ to the *ab* plane are difficult to prepare and almost certainly break during the first cool-down.

Note, that all three transverse Hall components are, within the measurement accuracy, identical with respect to magnitude and sign at $T\geq 240$ K. This means that $SrAs_3$ behaves as though it were cubic at these temperatures with respect to its Hall effect. This behavior is a clear indication that the "electrically monoclinic" properties of $SrAs_3$ are caused by the gradual appearance of a second band of charge carriers (holes) at temperatures <140 K. Evidence for monoclinic electronic properties of $SrAs_3$ at low temperatures has already been given with the determination of a nonellipsoidal Fermi surface of holes from Shubnikov—de Haas oscillations in the magnetoresistivity.[6]

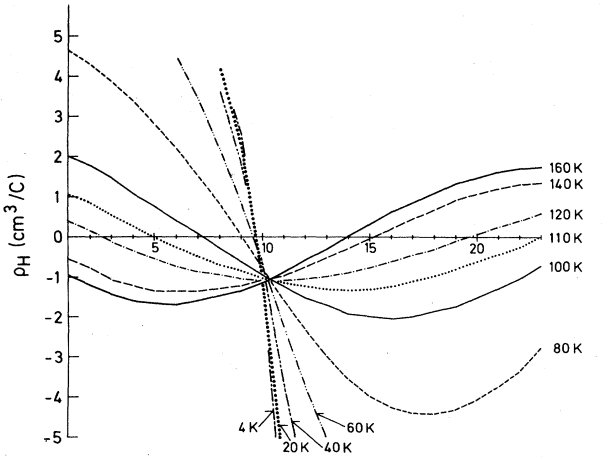

FIG. 9. Angular dependences of (THE + LHE) Hall coefficient for a sample with orientation III (see Fig. 2) pointing out the occurrence of a peculiar fixed point.

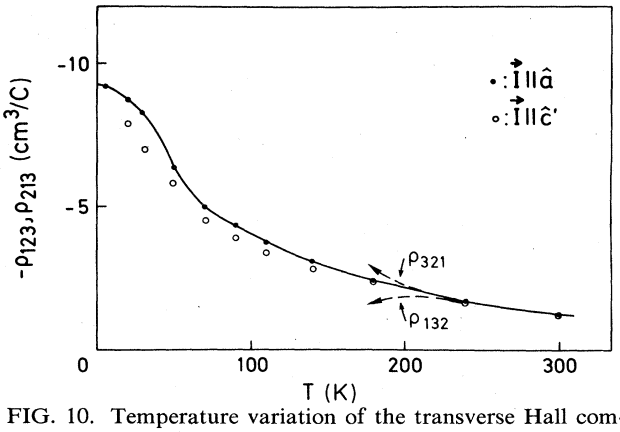

FIG. 10. Temperature variation of the transverse Hall component ρ_{213} $(=-\rho_{123})$ measured for two differently oriented samples: $\mathbf{I}\|\hat{\mathbf{a}}$ and $\mathbf{I}\|\mathbf{c}'$. The arrows symbolize the directions of deviation of ρ_{321} and ρ_{132} from ρ_{213} for $T<240$ K.

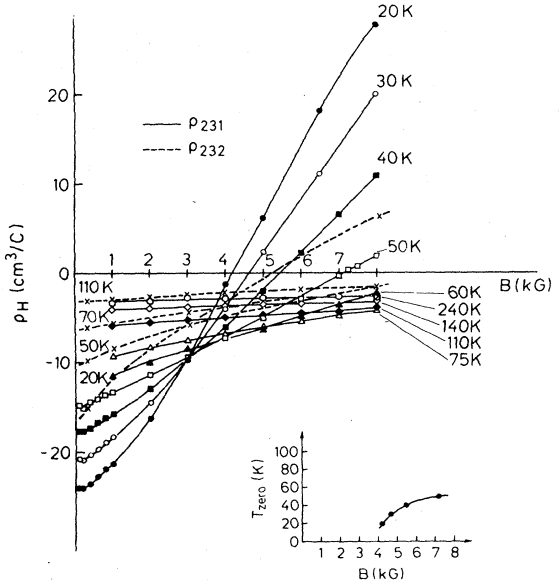

FIG. 11. Magnetic field dependences of transverse and longitudinal Hall components, ρ_{231} and ρ_{232}, for different temperatures. The inset depicts the zero crossings of the transverse component ρ_{231} as a function of magnetic field strength.

E. Magnetic field dependence of Hall components

The variation of ρ_{231} with magnetic field (Fig. 11) strongly resembles the case of a p-type conductor ($p > n$) with an electron mobility μ_n much larger than the hole mobility μ_p:[7]

$$\mu_n \gg \mu_p \ .$$

Denoting electron and hole concentrations by n and p, the Hall coefficient in the weak-field limit,

$$R(B\to 0)=-\frac{\mu_n^2 n-\mu_p^2 p}{|e|(\mu_n n+\mu_p p)^2} \ , \tag{4}$$

will be negative and crosses over to positive values, when it approaches the high-field limit,

$$R(B\to\infty)=-\frac{1}{|e|(n-p)} \ . \tag{5}$$

The Hall coefficient crossover moves to higher temperatures as the magnetic field is increased. Frequently cited examples of such a behavior are the early observations of Howarth, Jones, and Putley[8] in p-type InSb. In comparison, the corresponding longitudinal component ρ_{232} is less field dependent than ρ_{231} and shows a field-induced sign reversal at lower temperature.

The Hall component ρ_{132} however reveals a different magnetic field dependence, since in the temperature interval from 115 K to 90 K it crosses over from negative to positive values for *all* fields ≤ 8 kG. For $T < 90$ K, ρ_{132} stays positive for all magnetic fields. Now, it is only the corresponding longitudinal component which, at low temperatures, shows sign reversals with increasing magnetic field. With respect to their magnetic field dependences, transverse and longitudinal components change their roles for the orientations I and III.

Figure 12 shows the temperature variations of ρ_{231} and

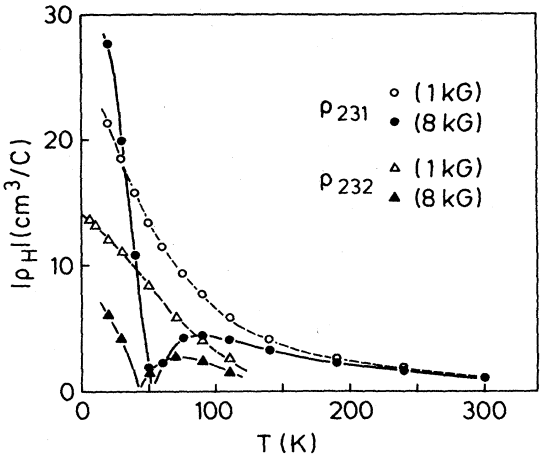

FIG. 12. Temperature variation of transverse and longitudinal Hall components, ρ_{231} and ρ_{232}, representative for the low-field (1-kG) and the intermediate-field (8-kG) case.

ρ_{232} for small (1 kG) and large (8 kG) magnetic fields. The curves for 8 kG correspond to Fig. 1 of paper I, and it can be verified from Fig. 11 of this work that 8 kG represents a typical intermediate-field case far away from either low-field or high-field saturation. A representative low-field curve is $\rho_{231}(T)$ for 1 kG. As stated above, the longitudinal component ρ_{232} has a weaker dependence on B, thus allowing 8 kG values (as done in paper I) still to be taken as representative for the temperature dependence of the low-field case for $T > 70$ K.

V. MODEL CALCULATION FOR A LHE

A. One-band model

A nonvanishing LHE component can probably be derived from a single nonellipsoidal band. Here, I follow a simpler approach for the calculation of a LHE component which is based on the assumption of an energy-independent relaxation time τ and the inclusion of an off-diagonal conductivity σ_{12} which is symmetry-allowed in a monoclinic crystal system. This idea has already been sketched in paper I. The velocity $\mathbf{v}$ of carriers under the influence of an electric field $\mathbf{E}$ and a magnetic field $\mathbf{B}$ is then given by

$$\mathbf{v}=\underline{\mu}(\mathbf{E}+\mathbf{v}\times\mathbf{B}) \ . \tag{6}$$

The mobility tensor $\underline{\mu}$ is related to the conductivity tensor $\underline{\sigma}$ via the carrier density n:

$$\underline{\sigma}=ne\underline{\mu} \ . \tag{7}$$

Applying the magnetic field $\mathbf{B}$ in the y direction, $\mathbf{B}=(0,B,0)$, yields

$$\begin{pmatrix} v_1 \\ v_2 \\ v_3 \end{pmatrix} = \begin{pmatrix} \mu_{11} & \mu_{12} & 0 \\ \mu_{12} & \mu_{22} & 0 \\ 0 & 0 & \mu_{33} \end{pmatrix} \left[\begin{pmatrix} E_1 \\ E_2 \\ E_3 \end{pmatrix} + \begin{pmatrix} -v_3 B \\ 0 \\ v_1 B \end{pmatrix} \right] . \tag{8}$$

Solving this equation for $\mathbf{v}$ leads to

$$\mathbf{v}=\frac{1}{N}\begin{bmatrix}\mu_1 & \mu_{12} & -\mu_1\mu_3B\\ \mu_{12} & (N\mu_2-\mu_{12}^2\mu_3B^2) & -\mu_{12}\mu_3B\\ \mu_1\mu_3B & \mu_{12}\mu_3B & \mu_3\end{bmatrix}\mathbf{E}\,, \tag{9}$$

where $N=1+\mu_1\mu_3B^2$ and $\mu_{ii}=\mu_i$.

Multiplying the mobility tensor $\underline{\mu}$ with en gives the magnetic-field-dependent conductivity tensor $\underline{\sigma}(B)$:

$$\mathbf{j}=\underline{\sigma}(B)\mathbf{E}\,, \tag{10}$$

$$\underline{\sigma}(B)=\frac{1}{N}\begin{bmatrix}\sigma_1 & \sigma_{12} & -\sigma_1\mu_3B\\ \sigma_{12} & (N\sigma_2-\mu_{12}^2\sigma_3B^2) & -\mu_{12}\sigma_3B\\ \sigma_1\mu_3B & \mu_{12}\sigma_3B & \sigma_3\end{bmatrix}, \tag{11}$$

The conductivity tensor has to be inverted to obtain the transverse and longitudinal Hall components, ρ_{132} and ρ_{232},[9]

$$\underline{\rho}(B)=\underline{\sigma}(B)^{-1}\,, \tag{12}$$

$$\rho_{132}=\frac{\rho_{13}(B)}{B}=\frac{1}{B}\frac{\sigma_{31}^*(B)}{|\underline{\sigma}(B)|}\,, \tag{13}$$

and

$$\rho_{232}=\frac{\rho_{23}(B)}{B}=\frac{1}{B}\frac{\sigma_{32}^*(B)}{|\underline{\sigma}(B)|}\,. \tag{14}$$

$|\underline{\sigma}(B)|$ denotes the determinant of $\underline{\sigma}(B)$ and $\sigma_{ij}^*(B)$ stands for the adjoint of $\sigma_{ij}(B)$.

For the transverse component we find the well-known result for a single-electron band:

$$\rho_{132}^0=\rho_{132}=\frac{1}{en}\,. \tag{15}$$

Thus, the THE is not influenced by an off-diagonal conductivity σ_{12}. The main result is the vanishing of the longitudinal component ρ_{232} due to

$$\rho_{232}\sim\frac{\sigma_{32}^*(B)}{B}=-\frac{1}{N}(-\sigma_1\mu_{12}\sigma_3+\sigma_1\sigma_{12}\mu_3)$$
$$=-\frac{(en)^2}{N}(-\mu_1\mu_{12}\mu_3+\mu_1\mu_{12}\mu_3)\equiv 0\,. \tag{16}$$

Within a simple one-band model the occurrence of a LHE cannot be explained.

B. Two-band model

The extension of the above model to the case of two bands is straightforward. If properties related to band (1) and band (2) are denoted by corresponding superscripts, Eqs. (10) and (11) can be extended to[10]

$$\mathbf{j}=\mathbf{j}^{(1)}+\mathbf{j}^{(2)}=\underline{\sigma}^{(1)}(B)\mathbf{E}+\underline{\sigma}^{(2)}(B)\mathbf{E}=\underline{\sigma}(B)\mathbf{E}\,, \tag{17}$$

and

$$\underline{\sigma}(B)=\begin{bmatrix}\frac{\sigma_1^{(1)}}{N^{(1)}}+\frac{\sigma_1^{(2)}}{N^{(2)}} & \frac{\sigma_{12}^{(1)}}{N^{(1)}}+\frac{\sigma_{12}^{(2)}}{N^{(2)}} & -\left[\frac{\sigma_1^{(1)}\mu_3^{(1)}}{N^{(1)}}+\frac{\sigma_1^{(2)}\mu_3^{(2)}}{N^{(2)}}\right]B\\ \frac{\sigma_{12}^{(1)}}{N^{(1)}}+\frac{\sigma_{12}^{(2)}}{N^{(2)}} & \frac{[N^{(1)}\sigma_2^{(1)}-\sigma_3^{(1)}(\mu_{12}^{(1)}B)^2]}{N^{(1)}}+\cdots & -\cdots\\ \left[\frac{\sigma_1^{(1)}\mu_3^{(1)}}{N^{(1)}}+\frac{\sigma_1^{(2)}\mu_3^{(2)}}{N^{(2)}}\right]B & \left[\frac{\sigma_3^{(1)}\mu_{12}^{(1)}}{N^{(1)}}+\frac{\sigma_3^{(2)}\mu_{12}^{(2)}}{N^{(2)}}\right]B & \frac{\sigma_3^{(1)}}{N^{(1)}}+\frac{\sigma_3^{(2)}}{N^{(2)}}\end{bmatrix}, \tag{18}$$

using a notation in analogy to Eq. (9).

Transverse and longitudinal Hall components are again obtained by

$$\rho_{132}=\frac{\rho_{13}(B)}{B}=\frac{1}{B}\frac{\sigma_{31}^*(B)}{|\underline{\sigma}(B)|}\,, \tag{13a}$$

and

$$\rho_{232}=\frac{\rho_{23}(B)}{B}=\frac{1}{B}\frac{\sigma_{32}^*(B)}{|\underline{\sigma}(B)|}\,. \tag{14a}$$

For the isotropic case, $\sigma_1^{(i)}=\sigma_2^{(i)}=\sigma_3^{(i)}=\sigma_i$, $\sigma_{12}^{(i)}=0$, the transverse Hall component reduces to

$$\rho_{132}=\frac{\sigma_1^2R_1+\sigma_2^2R_2+\sigma_1^2\sigma_2^2R_1R_2(R_1+R_2)B^2}{(\sigma_1+\sigma_2)^2+\sigma_1^2\sigma_2^2(R_1+R_2)^2B^2}\,, \tag{19}$$

which is the well-known two-band Hall formula, originally given by Chambers[11] ($\mu_i=R_i\sigma_i$ has been used).

The essential feature of the monoclinic two-band case is the fact that it indeed yields a nonvanishing LHE due to the inclusion of nondiagonal conductivity elements, as can easily be derived from Eq. (18),

$$\rho_{232}\sim\frac{\sigma_{32}^*(B)}{B}=\left[\frac{\sigma_1^{(1)}}{N^{(1)}}+\frac{\sigma_1^{(2)}}{N^{(2)}}\right]\left[\frac{\sigma_3^{(1)}\mu_{12}^{(1)}}{N^{(1)}}+\frac{\sigma_3^{(2)}\mu_{12}^{(2)}}{N^{(2)}}\right]-\left[\frac{\sigma_{12}^{(1)}}{N^{(1)}}+\frac{\sigma_{12}^{(2)}}{N^{(2)}}\right]\left[\frac{\sigma_1^{(1)}\mu_3^{(1)}}{N^{(1)}}+\frac{\sigma_1^{(2)}\mu_3^{(2)}}{N^{(2)}}\right]$$
$$=\frac{1}{N^{(1)}N^{(2)}}(\mu_3^{(1)}-\mu_3^{(2)})(\sigma_1^{(2)}\sigma_{12}^{(1)}-\sigma_1^{(1)}\sigma_{12}^{(2)})\,. \tag{20}$$

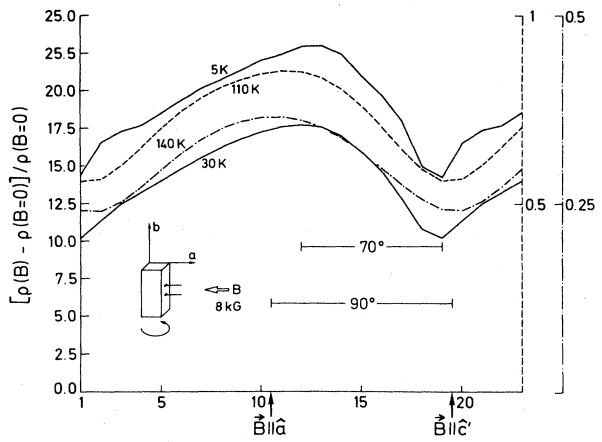

FIG. 13. Angular dependences of the transverse magnetoresistivity for a sample with $\mathbf{I}||\hat{\mathbf{b}}$ demonstrating the increasing asymmetry with respect to their maximal value for decreasing temperature. The measurements are made with steps of 10° for the rotation angle. Different scales are used for 5 and 30 K (0–25), 110 K (0–1), 140 K (0–0.5).

For $B\rightarrow 0$, which is the correct limit when the Hall tensor is defined as the linear term of the low-field expansion of $\underline{\rho}(B)$, the denominator of Eq. (14a) reduces to

$$|\underline{\sigma}(B=0)| = (\sigma_3^{(1)}+\sigma_3^{(2)})[(\sigma_1^{(1)}+\sigma_1^{(2)})(\sigma_2^{(1)}+\sigma_2^{(2)}) - (\sigma_{12}^{(1)}+\sigma_{12}^{(2)})^2] . \quad (21)$$

The last two relations, (20) and (21), lead to the final result for the low-field LHE:

$$\rho_{232}^0=\rho_{232}(B=0) = \frac{(\mu_3^{(1)}-\mu_3^{(2)})(\sigma_1^{(2)}\sigma_{12}^{(1)}-\sigma_1^{(1)}\sigma_{12}^{(2)})}{(\sigma_3^{(1)}+\sigma_3^{(2)})[(\sigma_1^{(1)}+\sigma_1^{(2)})(\sigma_2^{(1)}+\sigma_2^{(2)})-(\sigma_{12}^{(1)}+\sigma_{12}^{(2)})^2]} . \quad (22)$$

This result clearly demonstrates that a monoclinic two-band conductor can show a nonvanishing LHE, if the products of nondiagonal and diagonal conductivity elements (within the monoclinic *ac* plane) *and* the mobilities along the twofold axis *differ* for the two bands involved. With band (1) and band (2) containing electrons and holes, respectively, the second condition is necessarily fulfilled, since $\mathrm{sgn}(\mu^{(1)})=-\mathrm{sgn}(\mu^{(2)})$ in this case. Note, that σ is independent of the charge-carrier sign.

C. Experimental evidence for a two-band effect

Our knowledge of the properties of $SrAs_3$ is insufficient to make a realistic estimate of the LHE from Eq. (22) using experimentally determined values. Nevertheless, our experimental results suggest that, at least in $SrAs_3$, the LHE might be a two-band effect. We have to remember that the LHE strongly increases at temperatures below ~ 140 K. Three other observations are made in this temperature range.

(i) The three independent transverse Hall components which are almost identical and *n* type at room temperature start to diverge drastically.

(ii) The transverse component ρ_{132} changes sign at ~ 115 K in the low-field limit indicating the emergence of a hole band. At lower temperatures, the two other transverse components cross over from negative to positive values as a function of magnetic field.

(iii) The transverse magnetoresistivity with $\mathbf{I}||\hat{\mathbf{b}}$ being symmetric with respect to its maximum for $\mathbf{B}||\hat{\mathbf{a}}$ at higher temperatures shows increasing asymmetry for $T<140$ K (see Fig. 13). In contrast, the magnetoresistivities with $I||a$ and $I\perp ab$ remain symmetric down to the lowest temperatures.[12] This demonstrates again, as already stated in Sec. IV D, the increasing "electrically monoclinic" character of $SrAs_3$ with decreasing temperature.

VI. SUMMARY

I have complemented our recent observation of a LHE in $SrAs_3$ by a comprehensive study of this effect. All selection rules, imposed either by the Onsager relations or by symmetry, are found to be perfectly fulfilled. Precise results are obtained due to an improved method of measuring the LHE by rotating the samples with respect to the magnetic field. There is strong evidence that the LHE in $SrAs_3$ is a two-band effect. This evidence is based on the temperature dependence of the LHE components together with the temperature variation of the transverse components, their magnetic field dependence at low temperatures and the orientational dependence of the transverse magnetoresistivity as a function of temperature. I have shown that a simple two-band model including an off-diagonal conductivity term, which is symmetry allowed for a monoclinic space group, indeed yields a nonvanishing LHE. It should be pointed out, however, that within a more sophisticated model a single hole band with monoclinic Fermi surface would also lead to first-order LHE components.

As a concluding remark I would like to state that working with low-symmetry crystals can be rather tedious since one has to handle a large number of indices. In certain cases this hardship may be compensated by the observation of new and surprising effects.

ACKNOWLEDGMENTS

I acknowledge former cooperation with Dr. M. Möllendorf who originally had the idea of looking for a LHE in $SrAs_3$. Encouraged by the optimism of Professor H. J. Queisser, I continued this work to overcome the inconsistencies contained in our preliminary results. In addition, I have to thank P. Rudolf and R. Geiger for preparing the crystals, Monika Latzko for cutting, lapping, and orienting the samples, Dr. K. Peters for his determination of the *c* axis, M. Hafendörfer for setting up the excellent hardware of the Hall apparatus, K. Graf for his valuable tips in programming, and Jasmin Welskop for carefully putting contacts on the samples and her technical assistance in the measurements. Last but not least my thanks are due to Dr. M. Altarelli for his short but lucid introduction to the two-band model of conductivity.

[1]M. Möllendorf and W. Bauhofer, Phys. Rev. B **30**, 1099 (1984).
[2]W. Bauhofer, M. Wittmann, and H. G. von Schnering, J. Chem. Phys. Solids **42**, 687 (1981).
[3]A. C. Smith, J. F. Janak, and R. B. Adler, *Electronic Conduction in Solids* (McGraw-Hill, New York, 1967), p. 241.
[4]L. Onsager, Phys. Rev. **37**, 405 (1931); **38**, 2265 (1931).
[5]The transverse component ρ_{213} describes in our notation the usual textbook geometry for a Hall effect: $\mathbf{U}_H||\hat{\mathbf{y}}$, $\mathbf{I}||\hat{\mathbf{x}}$, $\mathbf{B}||\hat{\mathbf{z}}$.
[6]B. L. Zhou, E. Gmelin, and W. Bauhofer, Solid State Commun. **51**, 757 (1984).
[7]A. C. Beer, in *The Hall Effect and its Applications,* edited by C. L. Chien and C. R. Westgate (Plenum, New York, 1980), p. 323.
[8]D. Howarth, R. Jones,and E. Putley, Proc. Phys. Soc. London, Sect. B **70**, 124 (1957).
[9]It is mathematically easier to change the current direction while, in experiment, the magnetic field is rotated with respect to the sample orientation.
[10]See, for example, J. M. Ziman, *Principles of the Theory of Solids* (Cambridge University Press, London, 1972) pp. 250ff.
[11]R. C. Chambers, Proc. Phys. Soc. London, Sect. A **65**, 903 (1952).
[12]Approximating the low-field magnetoresistivity by $\Delta\rho/\rho=\mu^2B^2$ gives $\mu\approx10^5$ cm^2/V s in good agreement with a mobility determined from $\mu=\rho_T/\rho$.